

doi: 10.12029/gc20190412

龚雪婧, 曾建辉, 曹殿华. 2019. 江西冷水坑矿床含矿花岗斑岩的Sr–Nd及锆石Hf–O同位素研究[J]. 中国地质, 46(4): 818–831.
Gong Xuejing, Zeng Jianhui, Cao Dianhua.. 2019. Sr–Nd and zircon Hf–O isotopic constraints on the petrogenesis of the ore–bearing granitic porphyry at Lengshuikeng, Jiangxi Province[J]. Geology in China, 46(4): 818–831(in Chinese with English abstract).

江西冷水坑矿床含矿花岗斑岩的Sr–Nd及锆石Hf–O同位素研究

龚雪婧^{1,2}, 曾建辉³, 曹殿华^{1,2}

(1. 中国地质科学院, 北京 100037; 2. 中国地质调查局—中国地质科学院地球深部探测中心, 北京 100037;
3. 江西省地质矿产勘查开发局九一大队, 江西 鹰潭 335000)

提要:江西冷水坑铅锌矿床是武夷成矿带北段的典型矿床, 矿区内含矿花岗斑岩锆石U–Pb年龄为(162.0 ± 2.0)Ma, 岩浆分异程度较高, 具有高SiO₂(69.46%~75.52%)、高K₂O(K₂O/Na₂O>3.22)、强过铝质(ASI=1.20~1.96)的特征。岩体发育较明显的Eu负异常, 富集强不相容元素Rb、Th、U, 而亏损高场强元素Ba、Sr、Nb、Ta、P、Ti。全岩同位素测试结果显示, 冷水坑含矿花岗斑岩具有极高的⁸⁷Sr/⁸⁶Sr初始比值(0.74005~0.76518)与低的ε_{Nd}值(-11.48~-10.78), 锆石Hf–O同位素测定值变化范围较小, ¹⁷⁶Hf/¹⁷⁷Hf介于0.282317~0.282460, 具有负的ε_{Hf(t)}值(-12.39~-7.62)和相对较高的δ¹⁸O值(7.23‰~8.81‰), 指示岩浆主要来自于成熟地壳, 可能起源于北武夷地区变质基底, 源岩为基底变质岩, 这可能与古太平洋板块俯冲形成的挤压背景下的地壳熔融有关。

关键词:Sr–Nd–Hf–O同位素; 花岗斑岩; 冷水坑; 武夷成矿带; 华南

中图分类号:P588.13; P597 文献标志码:A 文章编号:1000–3657(2019)04–0818–14

Sr–Nd and zircon Hf–O isotopic constraints on the petrogenesis of the ore–bearing granitic porphyry at Lengshuikeng, Jiangxi Province

GONG Xuejing^{1,2}, ZENG Jianhui³, CAO Dianhua^{1,2}

(1. Chinese Academy of Geological Sciences, Beijing 100037, China; 2. SinoProbe Center, Chinese Academy of Geological Sciences and China Geological Survey, Beijing 100037, China; 3. No. 912 Geological Party of Jiangxi Bureau of Geology and Mineral Exploration and Development, Yingtan 335001, Jiangxi, China)

Abstract: The Lengshuikeng lead–zinc deposit in Jiangxi Province is a typical deposit in the northern section of the Wuyi metallogenic belt. The zircon SHRIMP U–Pb age of the ore–bearing granite porphyry in the mining area is (162.0 ± 2.0) Ma. The granite porphyries are highly evolved, with high SiO₂ (69.46%~75.52%), high K₂O (K₂O/Na₂O>3.22) and strong peraluminous (ASI=1.20~1.96). The negative Eu anomalies of the rock mass are relatively strong, and enriched in LILE such as Rb, Th, and U, while the

收稿日期:2019–04–18; 改回日期:2019–06–10

基金项目:中国地质调查局项目(DD20160082, DD20190012)、国家自然科学基金(41802097)及国家重点研发计划“深地资源勘查开采”重点专项(2016YFC0600201)联合资助。

作者简介:龚雪婧,女,1988年生,博士,助理研究员,主要从事岩石地球化学及矿床学研究;Email:xuejinggong@cags.ac.cn。

HFSE such as Ba, Sr, Nb, Ta, P, and Ti are depleted. In this study, the authors also report Sr–Nd and zircon Hf–O isotopic compositions of the granitic porphyries at Lengshuikeng. The results show that the granitic porphyries have relatively high initial $^{87}\text{Sr}/^{86}\text{Sr}$ ratios (0.74005~0.76518) and negative ϵNd values ($-11.48\sim-10.78$) as well as the zircon Hf–O isotope measurement value. The variation range of $^{176}\text{Hf}/^{177}\text{Hf}$ values (0.282317~0.282460) is small, with negative $\epsilon\text{Hf(t)}$ values ($-12.39\sim-7.62$) and relatively high $\delta^{18}\text{O}$ values ($7.23\text{\%}\sim8.81\text{\%}$), indicating that the magma mainly came from the mature crust, which may have originated from metamorphic basement of North Wuyi area, and the source rocks were probably the metamorphic basement. The magmatic activity was probably related to the crust melting under the compressive background formed by northwestward subduction of the Paleo-Pacific Plate.

Key words: Sr–Nd–Hf–O isotopes; granitic porphyry; Lengshuikeng; Wuyi metallogenic belt; Southeast China

About the first author: GONG Xuejing, female, born in 1988, doctor, assistant professor, engages in research on petrogeochemistry and economic geology; E-mail: xuejinggong@cags.ac.cn.

Fund support: Supported jointly by Project of China Geological Survey (No.DD20160082, No.DD20190012), National Natural Science Foundation (No. 41802097), National Key Research and Development Program (No. 2016YFC0600201).

1 引言

位于江西省贵溪市的冷水坑铅锌矿床,因具有典型的斑岩型矿床特征,被认为是一个超大型斑岩铅锌矿床(涂光炽, 1989; 孟祥金等, 2009)。前人对冷水坑矿床开展了大量的研究工作,包括矿床地质(孟祥金等, 2007; 何细荣等, 2010; 邱骏挺等, 2013; Wang et al., 2014)、含矿斑岩年代学及地球化学(孟祥金等, 2007, 2012; 左力艳等, 2010; 王长明等, 2011; 邱骏挺等, 2013; 苏慧敏等, 2013; 余明刚等, 2015)、矿床成因(孟祥金等, 2009; 周建祥, 2009; 何细荣等, 2010; 毛景文等, 2011; 王长明等, 2011; Wang et al., 2013)等。研究结果显示,空间上,铅锌矿化主要产出在花岗斑岩体内及其接触带附近,矿体产状与岩体一致;时间上,近年来高精度年代学研究获得冷水坑矿床含矿花岗斑岩的形成时代集中于155~163 Ma(左力艳等, 2010; 孟祥金等, 2012; 邱骏挺等, 2013; Wang et al., 2013),孟祥金等(2009)通过矿区蚀变岩绢云母Ar–Ar年龄测试获得的冷水坑矿床的形成时代为162.8 Ma,与花岗斑岩成岩年龄相一致。冷水坑矿床铅锌矿化与花岗斑岩体密切的时空关系,暗示两者可能具有密切的成因关联。因此,探究矿区花岗斑岩的岩浆源区特征,试图确定其成因机制,对于进一步正确理解花岗斑岩岩浆起源演化与Pb–Zn成矿可能存在的关系具有重要意义。

锆石是岩浆岩,尤其是中酸性岩中普遍存在的副矿物,其化学性质稳定、抗风化蚀变能力强,对

铪、氧同位素组成具有很好的保存性,因此锆石Hf–O同位素常用于约束岩浆源区特征、反演岩浆演化历史,是追踪岩浆物质来源及壳幔相互作用的重要工具(Mojzsis et al., 2001; Peck et al., 2001; Valley et al., 2005; Booth et al., 2005; Li et al., 2009, 2010; Cavosie et al., 2011; Grimes et al., 2013; Chen et al., 2015)。为此,本文在对冷水坑矿区含矿花岗斑岩开展了详细的年代学、岩石地球化学及Sr–Nd同位素地球化学研究的基础上,报道了冷水坑含矿花岗斑岩的锆石Hf–O同位素特征,试图对其物质来源及成因机制提供新的制约。

2 矿区地质特征及样品采集

冷水坑铅锌矿床位于江西省鹰潭市,产出于华夏板块北西缘,钦杭结合带南侧,受北北东向鹰潭—安远深断裂及北东向萍乡—绍兴深断裂控制(图1a);成矿带尺度上属于中国东部环太平洋成矿带内带,武夷银多金属成矿带北段。矿区基底地层为震旦系老虎塘组变质岩,盖层为矿区广泛分布的侏罗系—白垩系打鼓顶组和鹅湖岭组火山岩,打鼓顶组岩性为晶屑凝灰岩夹铁锰含矿层、安山岩、角砾安山岩及凝灰质粉砂岩、沉凝灰岩;鹅湖岭组岩性为晶屑凝灰岩、熔结凝灰岩并夹铁锰含矿层、凝灰质粉砂岩及流纹岩。矿区东北部零星出露石炭纪地层,岩性主要为石英细砂岩、砂岩、砂砾岩及紫红色粉砂岩。

矿区构造以断裂构造为主,主要表现为断层发育,其次变质基底及火山岩地层构成简单的褶皱构

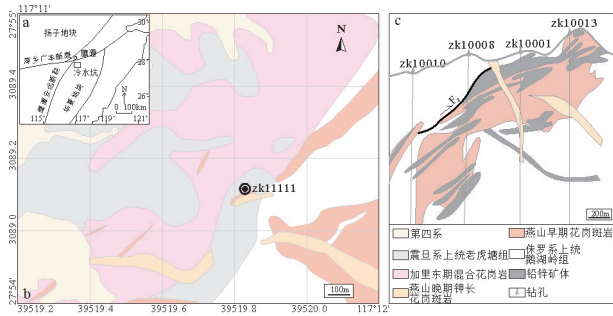


图1 冷水坑矿床区域构造简图(a)、冷水坑矿区地质简图(b)及100勘探线剖面图(c)(b,c据江西省地质矿产勘查开发局912地质队,1997)

Fig.1 Tectonic framework of the Lengshuikeng area (a), geological map of the Lengshuikeng deposit(b) and No.100 cross section(c)(b and c are modified after No.912 Geological Team of Geology and Mineral Resources Exploration Development Bureau of Jiangxi Province, 1997)

造。分布于矿区中部的 F_2 断裂(图1c),为一推覆构造,是区域推覆构造在矿区的出露部分,震旦系上统变质岩被该断裂推覆至侏罗系上统火山岩之上。总体走向北东45°,倾向北西,倾角15~35°,断裂破碎带宽数米至40 m左右,带内糜棱岩、断层角砾岩、碎裂岩及构造透镜体发育。断裂破碎带中见有硅化、绿泥石化、碳酸盐化、绢云母化、黄铁矿化及银铅锌矿化等。 F_2 断裂构造旁侧的次级派生断裂、裂隙较发育,展布方向有北东向、北北东向、近东西向、近南北向及北西向5组。派生断裂构造的延伸规模、位移均相对较小,但其与成矿关系比较密切,为重要的容矿储矿构造。花岗斑岩体与铅锌矿体的产状均明显受到近南北与近东西向两组断裂的控制,从而显示 F_2 断裂控制了岩体就位与储矿空间(图1c),由于 F_2 断裂上盘震旦系上统变质岩的良好封闭条件,含矿流体在屏蔽环境中得以进行充分交代、充填而成矿。

矿区内地质构造主要形成于加里东中晚期、燕山中期和燕山晚期。其中燕山中期岩浆活动强烈,主要形成浅成—超浅成的侵入岩体,岩性主要有花岗斑岩及石英正长斑岩;燕山晚期则主要形成流纹斑岩和钾长花岗斑岩,其岩体规模较小,主要呈岩脉、岩墙、岩瘤或岩盆产出,切割了较早形成的岩脉。与矿化关系密切的岩浆岩为花岗斑岩(图1b),分布于矿区的中部,自北西向南东呈不规则岩株状产出,出露总面积约为0.36 km²。

样品采集于冷水坑矿区银珠山矿田钻孔ZK11111中(图1b)。岩石样品较新鲜,呈浅灰色至浅灰绿色,块状构造,斑状结构,斑晶主要为石英和斜长石(15%~35%),粒径大小不一为0.5~5 mm,基质(65%~85%)多为显微花岗结构(图2)。主要矿物组成有斜长石(35%~45%)、石英(25%~30%)、钾长石(15%~20%),黑云母较少(1%~2%),副矿物见磷灰石、锆石等。

3 测试方法与结果

3.1 测试方法

样品由河北省诚信地质服务公司进行预处理,用于全岩主微量元素及Sr-Nd同位素测试的样品采用无污染法粉碎至200目,用于锆石U-Pb定年及Hf-O同位素分析的样品,将其破碎至100目以下,经淘洗后用电磁选和重液浮选方法选出重矿物,再在双目镜下挑选无明显裂痕且晶形和透明度较好的单颗粒锆石。挑选出的锆石样品在北京离子探针中心进行制靶及透射光、反射光和阴极发光(CL)显微照相。根据透射光、反射光和CL图像分析锆石颗粒内部显微结构特征,选择锆石内部无包裹体、无裂纹、阴极发光图像结构均匀或生长环带规则部位,进行原位U-Pb年龄及Hf-O同位素测定。

3.1.1 SHRIMP 锆石 U-Pb 定年

锆石SHRIMP U-Pb分析在北京离子探针中心SHRIMP II上完成。测试时一次流O⁻²强度为3~5 nA,束斑直径25~30 μm。标样M257(U=840×10⁻⁶, Nasdala et al., 2008)和TEM(年龄417 Ma, Black et al., 2003)分别用于锆石U含量和年龄校正。每分析3个样品点,分析一次标准锆石TEM进行同位素分馏校正,详细分析方法及原理见Williams(1998)。数据处理采用SQUID和ISOPLOT程序(Ludwig, 2001)。根据实测²⁰⁴Pb含量校正普通铅,采用²⁰⁶Pb/²³⁸Pb年龄为锆石年龄,同位素比值和单点年龄误差均为1σ。

3.1.2 主微量元素测试

主、微量元素分析在中国地质科学院国家地质实验测试中心完成,其中,主量元素含量采用X射线荧光光谱仪(XRF)测定,分析相对误差低于5%;稀土元素和微量元素采用等离子质谱(Excell)ICP-MS测定,分析相对误差低于10%。

3.1.3 Sr-Nd同位素测试

Sr-Nd同位素测试在南京大学内生金属矿床成矿机制研究国家重点实验室完成。将粉末样品烘干后称取约100 mg,完全溶解于HF+HNO₃混合酸中,采用Bio-Rad50WX8阳离子交换树脂法将Sr和Nd分离提纯出来。分离产物采用Thermo Finnigan公司的Triton TI热电离质谱仪(TIMS)进行Sr和Nd同位素比值测定,详细实验流程参见濮巍等(2004,2005)。Sr和Nd测定过程中质量分馏效应分别采用⁸⁶Sr/⁸⁷Sr=0.1194和¹⁴⁶Nd/¹⁴⁴Nd=0.7219进行校正。实验过程中国际标样NIST SRM987的⁸⁶Sr/⁸⁷Sr测定值为0.710259±4(2σ),与参考值0.710252±13(2σ)(Weis et al., 2006)在误差范围内一致;国际标样JNd的¹⁴⁶Nd/¹⁴⁴Nd测定值为0.512116±4(2σ),与参考值0.512115±7(2σ)(Tanaka et al., 2000)在误差范围内一致。

3.1.4 SHRIMP锆石O同位素测试

锆石O同位素分析在北京离子探针中心多接收二次离子质谱(SHRIMP II e-MC)上完成。在对锆石进行氧同位素测试之前,对已经进行过年龄测试的靶进行抛光,除去定年时形成的凹坑,使其平滑并消除可能存在的O污染,清洗烘干后在样品靶表面镀一层厚度约12 nm的Au膜。锆石O同位素原位测试分析点与U-Pb年龄测试分析点位置相同,以保证测得的O同位素值与年龄值相对应。测试采用的Cs⁺离子束约3.0 nA,通过10 kV加速电压轰击锆石样品表面,剥蚀斑束直径约20 μm,产生的二次¹⁶O⁻离子计数为10⁹ cps,经过30 eV能量过滤窗后,进入多接收器。每分析3个样品点分析1次标样锆石TEM($\delta^{18}\text{O}=8.2\text{\%}$)以确保仪器状态稳定,同

时对被测样品进行校正。 $\delta^{18}\text{O}$ 的分析结果以VSMOW为标准进行报道(‰),详细分析流程及原理见Ickert et al.(2008)。

3.1.5 LA-MC-ICP-MS锆石Hf同位素测试

锆石Hf同位素测试在中国地质科学院地质研究所LA-MC-ICP-MS实验室完成。实验仪器为Neptune Plus多接收等离子质谱仪和193 nm GeoLasPro激光发射器。实验过程中采用He作为剥蚀物质载气,剥蚀激光直径44 μm,测试位置采用U-Pb定年分析点原点测试。实验选用的锆石标样GJ-1作为参考物质,测试中锆石标准GJ-1的¹⁷⁶Hf/¹⁷⁷Hf加权平均值为0.282008±20。相关仪器运行条件及分析流程详见侯可军等(2007),Hf同位素计算公式参考吴福元等(2007)。

3.2 测试结果

3.2.1 锆石U-Pb年龄

本次工作采集冷水坑矿区银珠山矿段钻孔ZK11111中花岗斑岩样品,花岗斑岩样品中锆石为无色透明或浅黄色柱状,震荡环带特征明显(图3),测试样品中锆石Th/U比值均大于0.3(表1),与变质重结晶锆石Th/U比值(<0.1)差别较大,为岩浆成因(Hoskin and Black, 2000; Belousova et al., 2002),其年龄可以代表岩浆冷却结晶及岩体侵位的时代。测试获得花岗斑岩锆石加权平均年龄为(162.0±2.0)Ma(MSWD=1.4)(图3),Th、U含量均较高,分别为90×10⁻⁶~1337×10⁻⁶和137×10⁻⁶~3395×10⁻⁶,Th/U值介于0.36~0.88。

3.2.2 全岩主、微量元素及稀土元素组成

冷水坑花岗斑岩主量元素分析结果见表2,各主量元素含量从大到小为:SiO₂含量较高,为

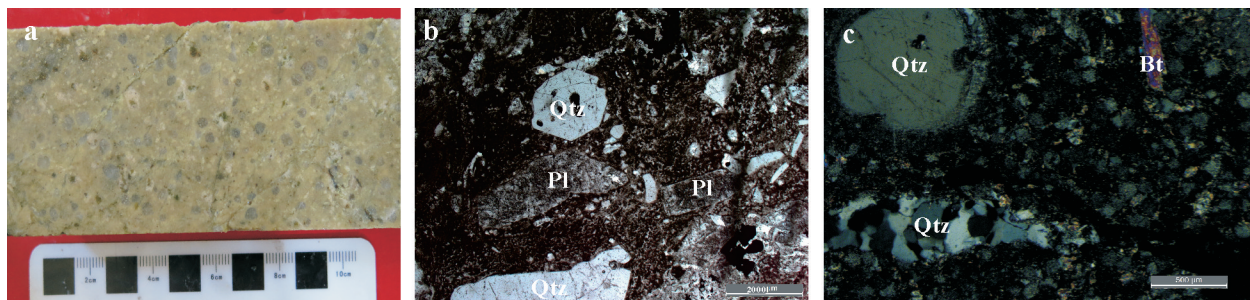


图2 冷水坑花岗斑岩样品矿物组合特征

Pl—斜长石; Qtz—石英; Bt—黑云母

Fig.2 Microscopic characteristics of the granite porphyry samples in the Lengshuikeng Pb-Zn mining area
Pl—Plagioclase; Qtz—Quartz; Bt—Biotite

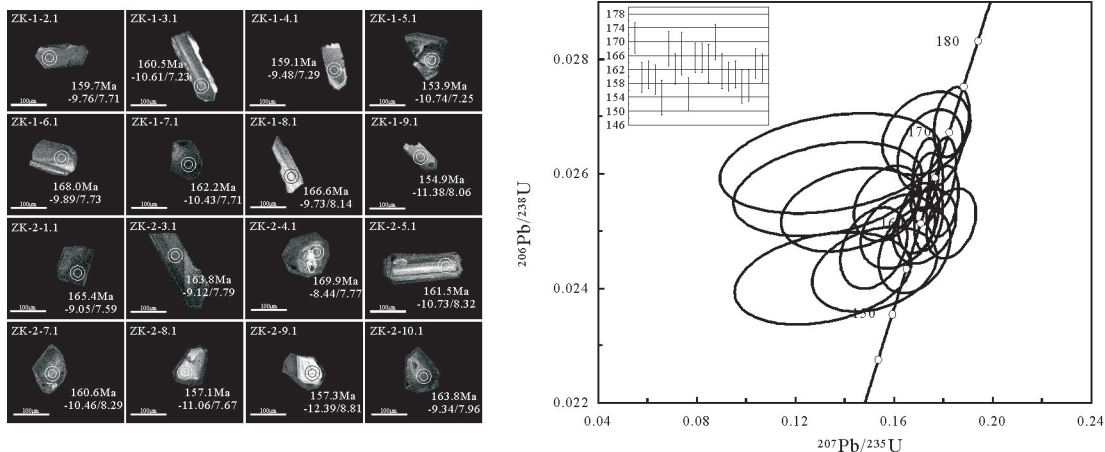


图3 冷水坑花岗斑岩锆石阴极发光图像、测试位置(小圆圈代表SHRIMP U-Pb和O同位素分析点,大圆圈代表LA-MC-ICP-MS Hf同位素分析点)和结果(分析点旁边的数字表示U-Pb年龄和 $\varepsilon_{\text{Hf}}(t)/\delta^{18}\text{O}$ 值)及SHRIMP锆石U-Pb协和图
Fig.3 Cathodoluminescence images of zircons from granite porphyry in the Lengshukeng Pb-Zn deposit with their data and the SHRIMP U-Pb concordia diagram

69.46%~75.52%, 平均值 73.27%; Al_2O_3 含量为 12.04%~14.07%, 平均值 13.07%; K_2O 为 4.99%~6.29%, 平均值 5.59%; FeO 为 0.84%~1.53%, 平均值 1.18%; Fe_2O_3 为 0.10%~2.30%, 平均值 0.83%; Na_2O 为 0.01%~1.64%, 平均值 0.65%; MgO 为 0.25%~0.90%, 平均值 0.55%; CaO 为 0.07%~1.68%, 平均值 0.54%; TiO_2 为 0.08%~0.30%, 平均值 0.20%; P_2O_5 为 0.02%~0.08%, 平均值 0.05%; 全碱含量即($\text{K}_2\text{O} + \text{Na}_2\text{O}$)为 5.04%~7.27%, 平均值 6.24%; 岩体显示出 K_2O 相对于 Na_2O 的强烈富集, $\text{K}_2\text{O}/\text{Na}_2\text{O}$ 比值介于 3.22~503.00, 平均值 103.34(表2)。在岩浆/火山岩系统全碱-硅(TAS)分类图(图4a)中, 花岗斑岩所有投点均位于花岗岩系中, 结合岩石手标本及镜下观察将其定名为花岗斑岩。在 $\text{SiO}_2-\text{K}_2\text{O}$ 图解(图4b)中, 花岗斑岩投点落入高钾钙碱性-钾玄岩系列区域; 里特曼指数($\sigma = (\text{Na}_2\text{O} + \text{K}_2\text{O})^2/(\text{SiO}_2 - 43)$)为 0.85~1.81(表2), 说明岩体均属于钙碱性系列。花岗斑岩铝饱和指数为 1.20~1.96, 显示出过铝质的特征, 在 ASI- SiO_2 图解(图4c)中, 数据点均落在强过铝质区域内。

花岗斑岩稀土元素总量(ΣREE)为 114.79×10^{-6} ~ 206.23×10^{-6} , 其中轻稀土元素总量(ΣLREE)为 101.24×10^{-6} ~ 194.33×10^{-6} , 重稀土元素总量(ΣHREE)为 11.90×10^{-6} ~ 14.13×10^{-6} , LREE/HREE 比值为 7.47~16.33(表2)。稀土元素球粒陨石标准化(Sun et al., 1989)配分曲线呈右倾平滑的平行曲

线簇(图5a), 富集轻稀土元素, $(\text{La}/\text{Yb})_N = 9.26 \sim 23.94$; 负 Eu 异常较强, δEu 为 0.42~0.67。总体上具有富集强不相容元素 Rb、Th、U, 而亏损高场强元素 Ba、Sr、Nb、Ta、P、Ti 的特点(图5b)。

3.2.3 全岩 Sr-Nd 同位素地球化学特征

冷水坑花岗斑岩具有较高含量的 Rb, 为 $235 \times 10^6 \sim 280 \times 10^6$, Sr 含量为 $33.2 \times 10^6 \sim 71.4 \times 10^6$, $(^{87}\text{Sr}/^{86}\text{Sr})_i$ 较高, 为 0.74005~0.76518(表3)。Sr 初始值比地壳部分熔融形成花岗岩的 Sr 初始值(0.719)更大(韩吟文等, 2003), 这种 Sr 同位素特征可能反映出花岗斑岩来源于地壳物质的熔融。 ε_{Nd} 值较低, 为 -11.48~-10.78, 二阶段模式年龄介于 1910~1828 Ma(表3)。

3.2.4 锆石 Hf-O 同位素地球化学特征

锆石 Hf-O 同位素测试结果见表4。结果显示冷水坑矿床花岗斑岩锆石的 Hf-O 同位素测定值相对较为集中, 且变化范围较小, $^{176}\text{Hf}/^{177}\text{Hf}$ 介于 0.282317~0.282460(表4), $\varepsilon_{\text{Hf}}(t) = -12.39 \sim -7.62$ ($t = 161$ Ma)(表4), 平均值为 -9.83, 相对应的二阶段模式年龄集中于 1697~1993 Ma(表4); $\delta^{18}\text{O} = 7.23\text{\textperthousand}$ ~8.81%(表4), 平均值为 7.83‰, 其累积频数直方图呈明显单峰分布特征(图6)。

4 讨 论

4.1 岩浆源区特征

冷水坑花岗斑岩总体上具有富集强不相容元

表1 冷水坑矿床花岗斑岩锆石SHRIMP U-Pb年龄分析结果
Table 1 Results of zircon U-Pb SHRIMP dating of granite porphyry in the Lengshukeng Pb-Zn deposit

测点号	同位素比值						年龄/Ma								
	含量/ 10^{-6}	Th	U	Th/U	$^{207}\text{Pb}/^{206}\text{Pb}$	1σ	$^{207}\text{Pb}/^{235}\text{U}$	1σ	$^{206}\text{Pb}/^{238}\text{Pb}$	1σ	$^{207}\text{Pb}/^{206}\text{U}$	1σ	$^{206}\text{Pb}/^{238}\text{U}$	1σ	$^{208}\text{Pb}/^{232}\text{Th}$
ZK11111-1-1.1	979	1591	0.64	0.0494	2.1	0.1833	2.6	0.0269	1.5	167.6	48.8	171.1	2.6	164.9	3.2
ZK11111-1-2.1	156	441	0.37	0.0498	4.6	0.1723	4.9	0.0251	1.7	186.6	107.7	159.7	2.7	152.5	8.0
ZK11111-1-3.1	520	1271	0.42	0.0488	2.8	0.1698	3.2	0.0252	1.6	140.0	65.7	160.5	2.5	155.6	4.7
ZK11111-1-4.1	235	670	0.36	0.0469	5.9	0.1615	6.2	0.0250	1.7	43.0	141.5	159.1	2.7	132.0	9.8
ZK11111-1-5.1	102	174	0.61	0.0393	18.0	0.1310	18.0	0.0242	2.2	-395.9	478.0	153.9	3.3	142	15.2
ZK11111-1-6.1	219	539	0.42	0.0480	4.6	0.1746	5.0	0.0264	1.8	97.3	109.8	168.0	3.0	156.4	9.6
ZK11111-1-7.1	397	631	0.65	0.0447	5.4	0.1572	5.7	0.0255	1.7	-69.3	133.1	162.2	2.7	151.5	5.7
ZK11111-1-8.1	117	137	0.88	0.0371	22.0	0.1340	22.0	0.0262	2.2	-546.6	591.3	166.6	3.7	156	13.8
ZK11111-1-9.1	153	188	0.84	0.0455	11.0	0.1520	11.0	0.0243	2.0	-31.4	272.1	154.9	3.1	140.2	9.6
ZK11111-1-11.1	1337	3074	0.45	0.0501	1.2	0.1796	2.0	0.0260	1.6	199.8	27.3	165.4	2.6	164.3	3.1
ZK11111-2-1.1	1239	3395	0.38	0.0482	1.4	0.1727	2.1	0.0260	1.6	108.9	33.5	165.4	2.6	158.9	3.5
ZK11111-2-3.1	157	345	0.47	0.0375	19.0	0.1330	19.0	0.0257	2.1	-518.9	497.2	163.8	3.4	124	19.8
ZK11111-2-4.1	227	588	0.40	0.0469	6.6	0.1730	6.8	0.0267	1.8	43.1	157.7	169.9	3.0	157	10.7
ZK11111-2-5.1	316	404	0.81	0.0406	13.0	0.1420	13.0	0.0254	1.9	-311.6	327.2	161.5	3.1	149	10.0
ZK11111-2-6.1	256	584	0.45	0.0528	3.2	0.1831	3.6	0.0251	1.6	321.8	72.4	160.0	2.6	166.1	5.9
ZK11111-2-7.1	1178	1944	0.63	0.0500	1.5	0.1739	2.2	0.0252	1.5	193.8	35.9	160.6	2.4	142.3	2.8
ZK11111-2-8.1	90	144	0.64	0.0495	5.4	0.1682	5.7	0.0247	2.0	169.3	125.6	157.1	3.1	166.4	7.0
ZK11111-2-9.1	106	186	0.59	0.0446	5.6	0.1517	5.9	0.0247	1.9	-79.9	136.7	157.3	2.9	151.8	6.3
ZK11111-2-10.1	573	1046	0.57	0.0488	2.0	0.1732	2.5	0.0257	1.6	137.9	46.6	163.8	2.6	158.9	3.5
ZK11111-2-11.1	540	1078	0.52	0.0510	1.8	0.1795	2.4	0.0255	1.6	241.8	40.6	162.4	2.5	165.4	3.9

素 Rb、Th、U, 而亏损高场强元素 Ba、Sr、Nb、Ta、P、Ti 的特点, 近年来的研究显示, 岩石 Sr、Ba 亏损可能与岩浆演化过程中斜长石的分离结晶作用有关, Ti、P 的相对亏损可能与岩浆分异过程有关, 归因于铁钛氧化物、磷灰石的分离结晶。由于 Rb 通常在成熟

度高的地壳中富集, 而 Sr 通常富集于成熟度低、演化不充分的地壳中, 因此 Rb/Sr 比值能灵敏地反映其源区特征(王德滋等, 1993)。冷水坑花岗斑岩的 Rb/Sr 值介于 2.76~7.80, 平均值为 4.95, 远高于中国东部上地壳平均值(0.31, 高山等, 1999)和全球上

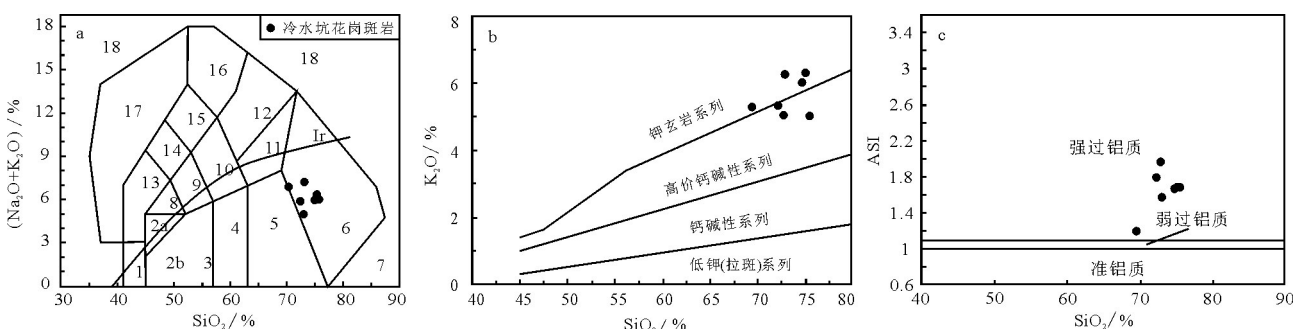


图4 岩石类型和系列划分图解

a— $\text{SiO}_2-(\text{Na}_2\text{O}+\text{K}_2\text{O})$ 图解(分类据 Wilson, 1989): 1—橄榄辉长岩; 2a—碱性辉长岩; 2b—亚碱性辉长岩; 3—辉长闪长岩; 4—闪长岩; 5—花岗闪长岩; 6—花岗岩; 7—硅英岩; 8—二长辉长岩; 9—二长闪长岩; 10—二长岩; 11—石英二长岩; 12—正长岩; 13—副长石辉长岩; 14—副长石二长闪长岩; 15—副长石二长正长岩; 16—副长石正长岩; 17—副长石深成岩; 18—霓方钠岩/磷霞岩/粗白榴岩); b— $\text{SiO}_2-\text{K}_2\text{O}$ 图解(据 Le Maitre, 2002); c—ASI— SiO_2 图解

Fig.4 Classification and series of diagrams of the granite porphyries

a— $\text{SiO}_2-(\text{Na}_2\text{O}+\text{K}_2\text{O})$ diagram (after Wilson, 1989): 1—Olivine gabbro; 2a—Alkaline gabbro; 2b—Subalkaline gabbro; 3—Gabbro diorite; 4—Diorite; 5—Granodiorite; 6—Granite; 7—Quartzolite; 8—Monzogabbro; 9—Monzodiorite; 10—Monzonite; 11—Adamellite; 12—Syenite; 13—Parafeldspar gabbro; 14—Parafeldspar monzodiorite; 15—Foid monzosyenite; 16—parafeldspar syenite; 17—parafeldspar plutonic rocks; 18—Tawite/ urtite/ italite); b— $\text{SiO}_2-\text{K}_2\text{O}$ diagram (after Le Maitre, 2002); c—ASI— SiO_2 diagram

表2 冷水坑铅锌矿床花岗斑岩主量(%)、稀土及微量元素(10^6)分析结果

Table 2 Major, rare earth and trace element compositions of granite porphyry in the Lengshuikeng Pb-Zn deposit

样品号	ZK11111-120.1	ZK11111-120.2	ZK11111-124.1	ZK11111-126.1	ZK11111-158	ZK11111-162.6	ZK11111-200.3
SiO ₂	75.52	72.23	74.75	72.82	69.46	72.97	75.16
TiO ₂	0.18	0.19	0.18	0.19	0.28	0.30	0.08
Al ₂ O ₃	12.93	12.86	13.05	12.79	13.74	14.07	12.04
Fe ₂ O ₃	0.10	2.30	0.41	0.82	0.54	0.11	1.52
FeO	1.24	0.84	1.06	1.53	1.28	1.35	0.95
MnO	0.57	0.46	0.59	1.13	0.49	0.24	0.16
MgO	0.49	0.47	0.54	0.68	0.90	0.50	0.25
CaO	0.26	0.20	0.69	0.58	1.68	0.27	0.07
Na ₂ O	1.09	0.63	0.04	0.01	1.64	1.04	0.13
K ₂ O	4.99	5.32	5.99	5.03	5.28	6.23	6.29
P ₂ O ₅	0.05	0.05	0.05	0.05	0.08	0.08	0.02
Al ₂ O ₃ /TiO ₂	71.83	67.68	72.50	67.32	49.07	46.90	150.50
LOI	2.44	3.38	2.68	3.56	3.56	2.22	2.42
Mg [#]	0.40	0.22	0.40	0.35	0.48	0.38	0.16
K ₂ O+Na ₂ O	6.08	5.95	6.03	5.04	6.92	7.27	6.42
K ₂ O/Na ₂ O	4.58	8.44	149.75	503.00	3.22	5.99	48.38
里特曼指数	1.14	1.21	1.15	0.85	1.81	1.76	1.28
ASI	1.69	1.80	1.67	1.96	1.20	1.57	1.68
La	33.90	33.70	30.80	38.30	41.40	48.40	23.50
Ce	61.80	62.60	57.80	71.70	77.90	90.80	44.90
Pr	7.61	7.84	7.15	8.46	9.28	10.60	5.83
Nd	27.20	26.90	24.90	29.40	34.20	36.90	21.20
Sm	5.58	5.40	4.95	5.86	6.18	6.62	5.15
Eu	0.74	1.10	0.75	0.86	0.89	1.01	0.66
Gd	4.25	4.30	4.23	4.55	4.23	4.19	4.18
Tb	0.61	0.57	0.56	0.66	0.58	0.56	0.65
Dy	3.46	3.46	3.39	3.97	3.36	3.17	3.85
Ho	0.61	0.57	0.63	0.67	0.58	0.58	0.68
Er	1.71	1.67	1.77	1.88	1.75	1.49	1.82
Tm	0.27	0.24	0.26	0.29	0.26	0.24	0.28
Yb	1.75	1.68	1.76	1.85	1.63	1.45	1.82
Lu	0.25	0.24	0.27	0.26	0.26	0.22	0.27
Rb	242.00	235.00	276.00	259.00	224.00	280.00	249.00
Ba	617.00	619.00	650.00	457.00	782.00	982.00	671.00
Th	21.60	22.40	21.50	22.40	22.90	25.20	21.90
U	5.93	5.18	4.71	6.90	4.97	4.95	6.56
Nb	18.90	19.10	18.40	19.80	17.90	17.90	21.70
Ta	1.73	1.79	1.77	1.81	1.56	1.52	2.17
Sr	60.60	48.50	40.80	33.20	81.20	71.40	54.40
Zr	106.00	99.40	103.00	110.00	126.00	140.00	68.30
Hf	3.67	3.83	3.83	3.90	4.22	4.50	3.17
Y	17.40	15.80	17.90	19.40	16.90	15.10	17.50
Rb/Sr	3.99	4.85	6.76	7.80	2.76	3.92	4.58
Sr/Ba	0.10	0.08	0.06	0.07	0.10	0.07	0.08
Nb/Ta	10.92	10.67	10.40	10.94	11.47	11.78	10.00
Zr/Hf	28.88	25.95	26.89	28.21	29.86	31.11	21.55
Σ REE	149.74	150.27	139.22	168.71	182.50	206.23	114.79
LREE/HREE	10.60	10.80	9.82	10.94	13.43	16.33	7.47
La _N /Yb _N	13.90	14.39	12.55	14.85	18.22	23.94	9.26
δ Eu	0.45	0.67	0.49	0.49	0.50	0.55	0.42
δ Ce	0.91	0.91	0.92	0.93	0.93	0.94	0.91

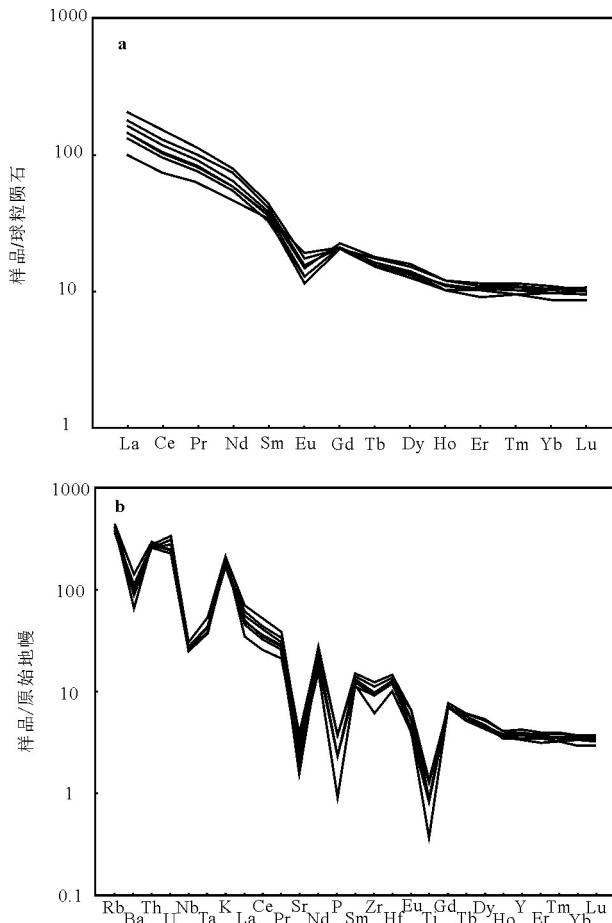


图5 稀土元素球粒陨石标准化配分曲线图(a)和微量元素原始地幔标准化配分曲线图(b)(球粒陨石、原始地幔数据据 Sun et al., 1989)

Fig.5 Chondrite-normalized REE patterns (a) and primitive mantle-normalized trace element patterns (b) (data of chondrite and primitive mantle after Sun et al., 1989)

地壳平均值(0.32, Taylor and McLennan, 1985)。此外,花岗斑岩Nb/Ta比值介于10.00~11.78,平均值为10.88,远低于中国东部上地壳平均值(16.2,高山等,1999)和全球上地壳平均值(12.0, Taylor and McLennan, 1985),这种较高的Rb/Sr比值和较低的Nb/Ta比值都指示其源区为成熟度较高的壳源物质,但还需同位素特征的进一步约束。

冷水坑花岗斑岩具有极高的Sr同位素特征值(0.74005~0.76518)和低的Nd同位素特征值(-11.48~-10.78),计算的二阶段模式年龄介于1910~1828 Ma,指示其源区为较老的壳源物质。在Sr-Nd同位素相关图中(图7),样品点全部位于华夏陆块古元古代变质基底区域内,表明物质主要来

自于成熟地壳,可能起源于北武夷地区变质基底,源岩为基底变质岩。冷水坑花岗斑岩锆石 $\delta^{18}\text{O}$ 值介于7.23‰~8.81‰,均值为7.87‰,除3颗锆石外(分别为7.23‰、7.25‰和7.29‰),其余锆石 $\delta^{18}\text{O}$ 值均高于太古宙岩浆锆石 $\delta^{18}\text{O}$ 值(6.5‰~7.5‰, Valley et al., 2005),暗示其岩浆来自于表壳物质。锆石较老的二阶段Hf模式年龄(1697~2024 Ma),也指示了成熟地壳物质的贡献。根据花岗斑岩全岩的SiO₂含量(73.27%)估算出全岩 $\delta^{18}\text{O}$ 值大致介于14.21‰~15.79‰($\delta^{18}\text{O}_{\text{Zn}} - \text{WR} = \delta^{18}\text{O}_{\text{Zrc}} - \delta^{18}\text{O}_{\text{WR}} \approx -0.0612 (\text{wt.\%SiO}_2) + 2.5$, Valley et al., 2005),高于全球典型S型花岗岩($\delta^{18}\text{O}=9.9\text{\%}\sim10.5\text{\%}$, O'Neil, 1977)的全岩氧同位素组成。在 $\varepsilon_{\text{Hf}}(t)-\delta^{18}\text{O}$ 二端元图解中(图8),冷水坑花岗斑岩锆石Hf-O同位素组成非常靠近但并未完全落入地壳(S型花岗岩)端元区,这样的同位素特征可能与侏罗纪岩浆活动来源于变质基底的熔融有关,加入的地幔物质可能是古老地壳中先存的火成岩(Chappell and Stephens, 1988; Sylvester, 1998; Clemens, 2003)。

4.2 地球动力学背景

由微量元素原始地幔标准化蛛网图(图5b)可以看出,冷水坑花岗斑岩总体上具有富集强不相容元素Rb、Th、U,而亏损高场强元素Ba、Sr、Nb、Ta、P、Ti的特点,其配分模式具有明显的Nb-Ta槽和Ti谷,表现出与俯冲相关的弧花岗岩的特征(Rogers et al., 1989; Stern, 2002)。在花岗岩类构造环境判别图(图9a,b)中,花岗斑岩样品均投点于同碰撞花岗岩或同碰撞花岗岩与弧花岗岩过渡范围内,指示其形成与板片俯冲、碰撞作用相关。在Zr/TiO₂-Ce/P₂O₅图解(图9c)中,样品点均落大陆弧范围内,由此推测花岗斑岩为产出在活动大陆边缘的陆缘弧岩浆岩。在Nb-Rb/Zr图解(图9d)中,绝大多数投点位于正常弧范围,少数位于成熟弧或正常弧与成熟弧过渡范围内,暗示花岗斑岩为正常弧向成熟弧环境过渡的岩浆产物(Brown, 1984)。

前人研究普遍认为华南地区白垩纪(晚燕山期)岩浆活动主要受到古太平洋板块俯冲的影响,发生于与之相关的活动大陆边缘环境,然而对于侏罗纪(燕山早期)岩浆活动的地球动力学过程尚存争议(Zhou et al., 2000; Li et al., 2007; Chen et al., 2008)。为进一步诠释侏罗纪华南板块内部的岩浆

表3 冷水坑铅锌矿床花岗斑岩Sr-Nd同位素分析结果

Table 3 Sr-Nd isotope compositions of granite porphyry in the Lengshuikeng Pb-Zn deposit

样品号	Rb/ 10^{-6}	Sr/ 10^{-6}	$^{87}\text{Rb}/^{86}\text{Sr}$	$^{87}\text{Sr}/^{86}\text{Sr}$	$^{87}\text{Sr}/^{86}\text{Sr(i)}$	Sm/ 10^{-6}	Nd/ 10^{-6}	$^{147}\text{Sm}/^{144}\text{Nd}$	($^{143}\text{Nd}/^{144}\text{Nd}$)t	$\varepsilon_{\text{Nd}}(t)$	T_{DM}/Ma	T_{DM2}/Ma
ZK11111-120.2	235	48.5	12.023	0.747	0.74454	5.4	26.9	0.121	0.512	-11.04	1908	1857
ZK11111-126.1	259	33.2	19.308	0.769	0.76518	5.86	29.4	0.120	0.512	-11.48	1928	1890
ZK11111-162.6	280	71.4	9.736	0.742	0.74005	6.62	36.9	0.108	0.512	-11.15	1703	1828
ZK11111-200.3	249	54.4	11.355	0.749	0.74655	5.15	21.2	0.147	0.512	-10.78	2541	1910

表4 冷水坑铅锌矿床花岗斑岩锆石原位Hf-O同位素组成

Table 4 Zircon in situ Hf-O isotopic composition of granite porphyry in the Lengshuikeng Pb-Zn deposit

测点号	$^{176}\text{Yb}/^{177}\text{Hf}$	$^{176}\text{Lu}/^{177}\text{Hf}$	$^{176}\text{Hf}/^{177}\text{Hf}$	2σ	$\varepsilon_{\text{Hf}}(t)$	T_{DM}/Ma	T_{DM2}/Ma	$\delta^{18}\text{O}/\text{‰}$	1σ	T/Ma
ZK11111-1-1.1	0.037879	0.001202	0.282434	0.000018	-8.34	1163	1747	—	—	171
ZK11111-1-2.1	0.041230	0.001317	0.282401	0.000016	-9.76	1213	1828	7.71	0.27	160
ZK11111-1-3.1	0.040955	0.001325	0.282376	0.000016	-10.61	1247	1882	7.23	0.19	161
ZK11111-1-4.1	0.036203	0.001203	0.282409	0.000015	-9.48	1198	1810	7.29	0.19	159
ZK11111-1-5.1	0.036567	0.001231	0.282376	0.000018	-10.74	1244	1886	7.25	0.31	154
ZK11111-1-6.1	0.036666	0.001162	0.282392	0.000015	-9.89	1220	1843	7.73	0.24	168
ZK11111-1-7.1	0.040912	0.001281	0.282380	0.000013	-10.43	1240	1872	7.71	0.25	162
ZK11111-1-8.1	0.012516	0.000421	0.282395	0.000015	-9.73	1193	1832	8.14	0.20	167
ZK11111-1-9.1	0.038456	0.001237	0.282358	0.000018	-11.38	1271	1927	8.06	0.23	155
ZK11111-1-11.1	0.059403	0.001878	0.282460	0.000016	-7.62	1146	1697	—	—	165
ZK11111-2-1.1	0.068686	0.002188	0.282420	0.000020	-9.05	1213	1787	7.59	0.30	165
ZK11111-2-3.1	0.043414	0.001372	0.282417	0.000017	-9.12	1192	1791	7.79	0.15	164
ZK11111-2-4.1	0.025488	0.000827	0.282431	0.000017	-8.44	1156	1753	7.77	0.19	170
ZK11111-2-5.1	0.034679	0.001085	0.282372	0.000015	-10.73	1246	1891	8.32	0.26	162
ZK11111-2-6.1	0.035441	0.001149	0.282412	0.000015	-9.33	1191	1801	—	—	160
ZK11111-2-7.1	0.046875	0.001510	0.282381	0.000017	-10.46	1247	1873	8.29	0.14	161
ZK11111-2-8.1	0.026586	0.000766	0.282364	0.000018	-11.06	1246	1909	7.67	0.20	157
ZK11111-2-9.1	0.015614	0.000510	0.282326	0.000017	-12.39	1291	1993	8.81	0.29	157
ZK11111-2-10.1	0.035758	0.001144	0.282410	0.000015	-9.34	1194	1805	7.96	0.24	164
ZK11111-2-11.1	0.056093	0.001768	0.282431	0.000016	-8.69	1185	1763	—	—	162

注:锆石原位O同位素测试单位为北京离子探针中心;原位Hf同位素测试单位为中国地质科学院地质研究所。

活动,许多构造模型被提出,如Charvet(2010)和Jiang(2011)提出的低角度俯冲模型,Hou et al.(2009)提出的陆内造山及造山后伸展作用模型,Gilder(1991)提出的伸展环境盆岭省模型,板内裂谷模型(Chen, 1999; Li 2000; Xie et al., 2006)。尽管存在一些争议,但大多数学者认为这些模型中的任何一种,都与古太平洋的平板俯冲相关(Martin et al., 1995; Lapierre et al., 1997; Zhou et al., 2012)。从构造演化历史看,本区在中生代属于中国东南大陆边缘体系,经历了三叠纪—中晚侏罗世(220~150 Ma)的陆内俯冲—陆内拼贴碰撞造山、晚侏罗世((145±5) Ma)由挤压向伸展扩张的转换、早白垩世

(125~105 Ma)的陆内扩张增强以及92 Ma开始的裂解阶段(孟祥金等,2007; Wang et al., 2013)。本次研究查明冷水坑含矿斑岩形成于162 Ma左右,处于陆内造山阶段的晚期,结合冷水坑含矿花岗斑岩的岩石地球化学特征,我们倾向性地认为冷水坑含矿花岗斑岩岩浆活动总体构造环境为古太平洋板块持续的俯冲与挤压,是古太平洋板块北西向俯冲引起的岩浆活动在北武夷地区的响应。

5 结 论

(1)冷水坑花岗斑岩分异程度较高,具有高SiO₂、高K₂O、强过铝质的特征。岩体发育较明显的

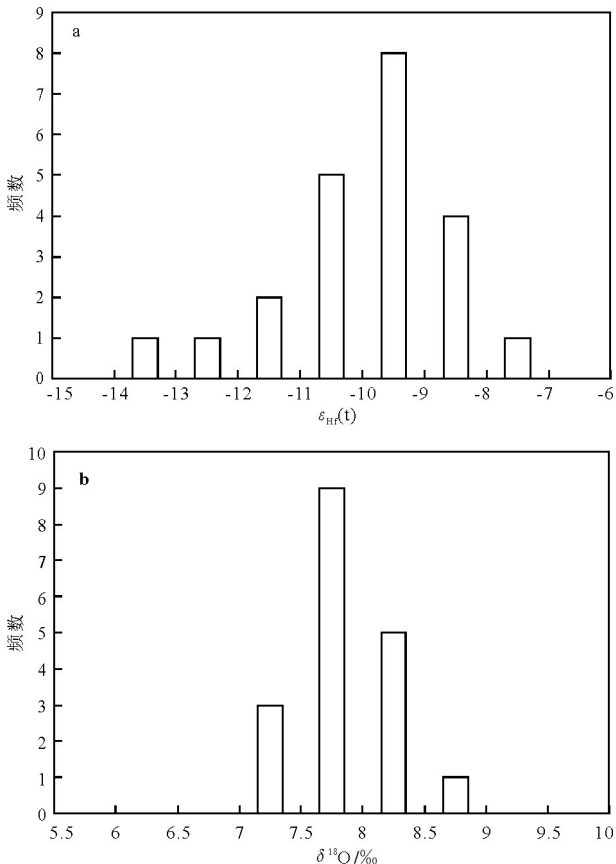


图6 冷水坑花岗斑岩锆石Hf同位素(a)和O同位素(b)组成
频数统计图

Fig.6 The cumulative probability histogram of in situ zircon $\epsilon_{\text{Hf}}(t)$ (a) and $\delta^{18}\text{O}$ (b) for the Lengshuikeng granite porphyries

Eu负异常,富集强不相容元素Rb、Th、U,而亏损高场强元素Ba、Sr、Nb、Ta、P、Ti。其配分模式具有明显的Nb-Ta槽和Ti谷,表现出与俯冲相关的弧花岗岩的特征。

(2)冷水坑含矿花岗斑岩SHRIMP U-Pb年龄为(162.0 ± 2.0)Ma,具有均一的锆石Hf-O同位素组成, $\epsilon_{\text{Hf}}(t) = -12.39 \sim -7.62$,均值 -9.83 ; $\delta^{18}\text{O} = 7.23\text{‰} \sim 8.81\text{‰}$,均值 7.83‰ ,且具有极高的 $^{87}\text{Sr}/^{86}\text{Sr}$ 初始比值($0.74005 \sim 0.76518$)与低的 ϵ_{Nd} 值($-11.48 \sim 10.78$)。指示岩浆主要来自于成熟地壳,可能起源于北武夷地区变质基底,源岩为基底变质岩。其岩浆活动总体构造环境为古太平洋板块持续的俯冲与挤压,是古太平洋板块北西向俯冲引起的岩浆活动在北武夷地区的响应。

致谢:野外工作中得到了江西省地质矿产勘查开发局九一大队工作人员的大力支持。中国地

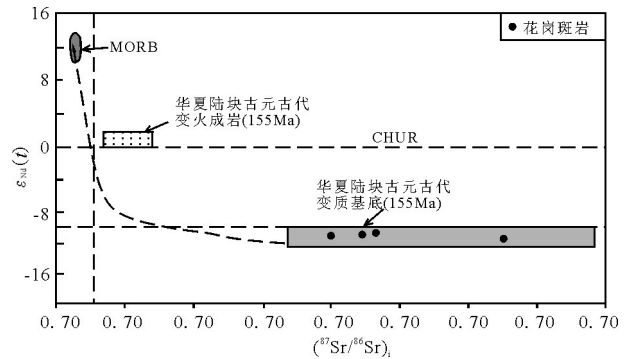


图7 冷水坑花岗斑岩 $\epsilon_{\text{Nd}}(t)$ – $(^{87}\text{Sr}/^{86}\text{Sr})_i$ (底图据 Wang et al., 2013)图解

Fig.7 $^{87}\text{Sr}/^{86}\text{Sr}$ versus $\epsilon_{\text{Nd}}(t)$ diagram (after Wang et al., 2013) showing the isotope signatures for the Lengshuikeng granite porphyry

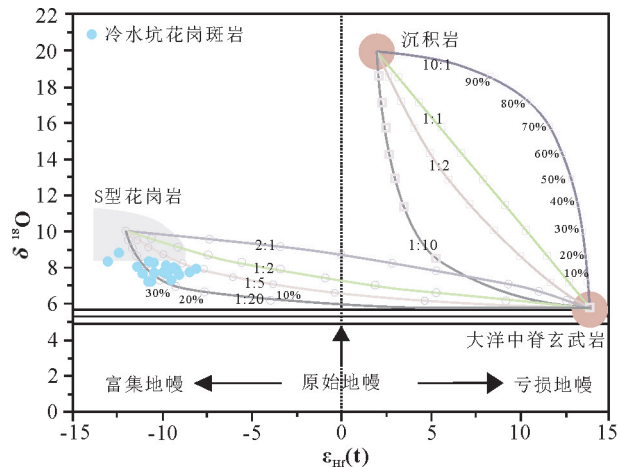


图8 冷水坑花岗斑岩锆石原位 $\epsilon_{\text{Hf}}(t)$ – $\delta^{18}\text{O}$ 关系图解
(不同端元Hf同位素数据据 Chauvel et al., 2008; O同位素数据据 Hoefs et al., 2009.MORB: $\delta^{18}\text{O}=5.8\text{‰}$, $\epsilon_{\text{Hf}}=13.9$; 沉积岩: $\delta^{18}\text{O}=20\text{‰}$, $\epsilon_{\text{Hf}}=2$; S型花岗岩: $\delta^{18}\text{O}=10\text{‰}$, $\epsilon_{\text{Hf}}=-12$)。混合线根据不同 $\text{Hf}_{\text{MORB}}/\text{Hf}_{\text{sediments}}$ (1:10~10:1) 和 $\text{Hf}_{\text{MORB}}/\text{Hf}_{\text{granites}}$ (1:2~20:1) 值做出, 线上空心圆圈/及正方形表示混合比例(10%间隔)

Fig.8 In-situ zircon $\delta^{18}\text{O}$ vs $\epsilon_{\text{Hf}}(t)$ isotope plot of the Lengshuikeng granite porphyry (hafnium isotope sources after Chauvel et al., 2008 and oxygen isotopes after Hoefs et al., 2009. The compositions of the members for mixing calculations are: MORB: $\delta^{18}\text{O}=5.8\text{‰}$, $\epsilon_{\text{Hf}}=13.9$; sediments: $\delta^{18}\text{O}=20\text{‰}$, $\epsilon_{\text{Hf}}=2$; S-type granites: $\delta^{18}\text{O}=10\text{‰}$, $\epsilon_{\text{Hf}}=-12$). The mixing curves were constructed using different $\text{Hf}_{\text{MORB}}/\text{Hf}_{\text{sediments}}$ and $\text{Hf}_{\text{MORB}}/\text{Hf}_{\text{granites}}$ elemental ratios from 1:10 to 10:1 and 1:2 to 20:1 respectively; the circles and squares on mixing curves are at 10% intervals

质科学院地质研究所潘小菲副研究员、张智宇副研究员在野外工作中给予了帮助,中国地质科学院的

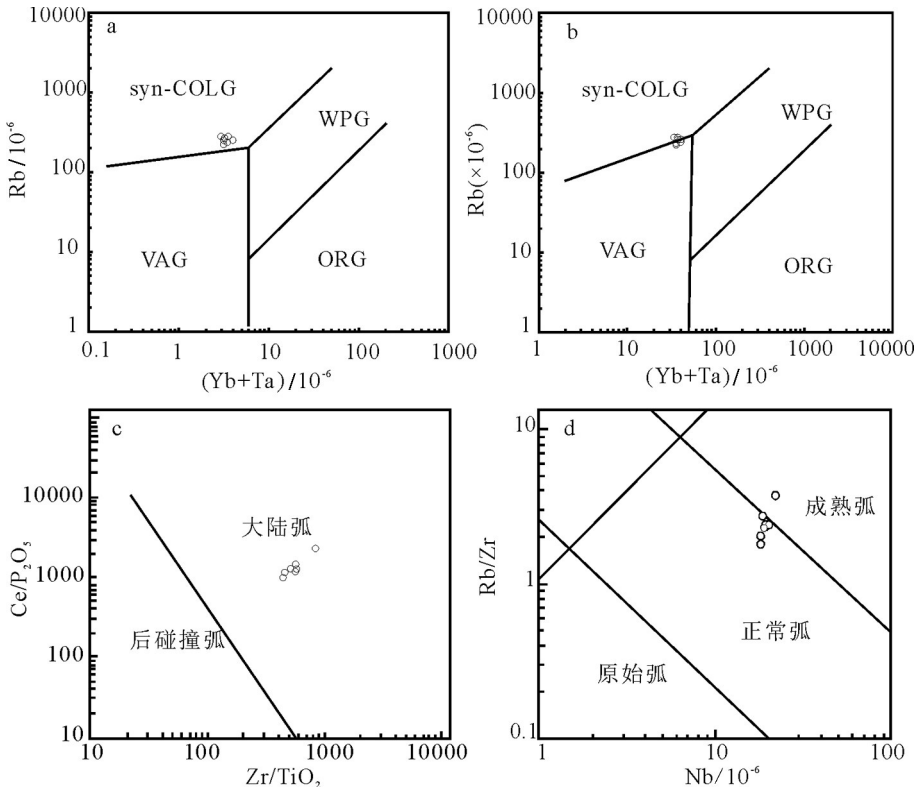


图9 冷水坑花岗斑岩构造环境判别图解(a,b,底图据 Pearce et al., 1984;c,底图据 Müller et al., 1992;d,底图据 Brown et al., 1988)

Fig.9 Tectonic setting discrimination diagrams of granite porphyry from the Lengshukeng Pb-Zn deposit(a, b, after Pearce et al., 1984; c, after Müller et al., 1992; d, after Brown et al., 1988)

赵苗博士、庄亮亮博士在测试和数据处理过程中给予了支持和帮助,在此一并表示衷心的感谢。

References

- Belousova E A, Griffin W L, O' Reilly S Y, Fisher N I. 2002. Igneous zircon: Trace element composition as an indicator of source rock type[J]. Contributions to Mineralogy and Petrology, 143(5): 602–622.
- Black L P, Kamo S L, Allen C M, Aleinikoff J N, Davis D W, Korsch R J, Foudoulis C. 2003. TEMORA 1: A new zircon standard for Phanerozoic U-Pb geochronology[J]. Chemical Geology, 200(1–2): 155–170.
- Booth A L, Kolodny Y, Chamberlain C P, McWilliams M, Schmitt A K, Wooden J. 2005. Oxygen Isotopic Composition and U-Pb Discordance in Zircon[J]. Geochimica et Cosmochimica Acta, 69 (20): 4895–4905.
- Brown C G, Thorpe R S, Webb P C. 1984. The geochemical characteristics of granitoids in contrasting arcs and comments on magma sources[J]. Journal of the Geological Society, 141(3): 411–426.
- Brown C G, Thorpe R S, Webb P C. 1984. The geochemical characteristics of granitoids in contrasting arcs and comments on magma sources[J]. Journal of the Geological Society, 141(3): 411–426.
- characteristics of granitoids in contrasting arcs and comments on magma sources[J]. Journal of the Geological Society, 141(3): 411–426.
- Cavosie A J, Valley J W, Kita N T, Spicuzza M J, Ushikubo T, Wilde S A. 2011. The origin of high $\delta^{18}\text{O}$ zircons: Marbles, megacrysts, and metamorphism[J]. Contributions to Mineralogy and Petrology, 162 (5): 961–974.
- Chappell B W, Stephens W E. 1988. Origin of infracrustal (I-type) granite magmas[J]. Earth and Environmental Science Transactions of the Royal Society of Edinburgh, 79(2): 71–86.
- Charvet J, Shu L S, Faure M, Choulet F, Wang B, Lu H F, Breton N L. 2010. Structural development of the Lower Paleozoic belt of South China: Genesis of an intra-continental orogen[J]. Journal of Asian Earth Science, 39:309–330.
- Chauvel C, Lewin E, Carpentier M, Anrdt N T, Marini J C. 2008. Role of recycled oceanic basalt and sediment in generating the Hf-Nd Mantle Array[J]. Nature Geoscience, 1: 64–67..
- Chen A. 1999. Mirror-image thrusting in the South China orogenic belt: Tectonic evidence from western Fujian, southeastern China[J]. Tectonophysics, 305: 497–519.
- Chen C H, Lee C Y and Shinjo R. 2008. Was there Jurassic Paleo-Pacific subduction in South China?: Constraints from $^{40}\text{Ar}/^{39}\text{Ar}$

- dating, elemental and Sr–Nd–Pb isotopic geochemistry of the Mesozoic basalts[J]. *Lithos*, 106: 83–92.
- Chen Yaping, Wei Chunjing, Zhang Jinrui, Chu Hang. 2015. Metamorphism and zircon U–Pb dating of garnet amphibolite in the Baoyintu Group, Inner Mongolia[J]. *Science Bulletin*, 60(19): 1698–1707.
- Clemens J D. 2003. S-type granitic magmas—petrogenetic issues, models and evidence[J]. *Earth Science Review*, 61: 1–18.
- Gilder S A, Keller G R, Luo M, Goode P C. 1991. Eastern Asia and the western Pacific timing and spatial distribution of rifting in China[J]. *Tectonophysics*, 197: 225–243.
- Grimes C B, Ushikubo T, Kozdon R, Valley J W. 2013. Perspectives on the Origin of Plagiogranite in Ophiolites from Oxygen Isotopes in Zircon[J]. *Lithos*, 179: 48–66.
- Han Yinwen, Ma Zhendong. 2003. *Geochemistry*[M]. Beijing: Geological Publishing House, 1–370(in Chinese).
- Hoefs, J., 2009. *Stable Isotope Geochemistry*[M]. Berlin: Springer-Verlag, 1–286.
- Hoskin P W O, Black L P. 2000. Metamorphic Zircon Formation by Solid-State Recrystallization of Protolith Igneous Zircon[J]. *Journal of Metamorphic Geology*, 18(4): 423–439.
- Hou Kejun, Li Yanhe, Zou Tianren, Qu Xiaoming, Shi Yuruo, Xie Guiqing. 2007. Laser ablation–MC–ICP–MS technique for Hf isotope microanalysis of zircon and its geological applications[J]. *Acta Petrologica Sinica*, 23(10): 2595–2604(in Chinese with English abstract).
- Hou Zengqian, Yang Zhiming. 2009. Porphyry deposits in continental settings of China: Geological characteristics, magmatic hydrothermal system, and metallogenesis model[J]. *Acta Geologica Sinica*, 83:1781–1817.
- Ickert R B, Hiess J, Williams I S, Holden P, Ireland T R, Lane P, Schram N, Foster J J and Clement S W. 2008. Determining high precision, in situ, oxygen isotope ratios with a SHRIMP II: Analyses of MPI–DING silicate–glass reference materials and zircon from contrasting granites[J]. *Chemical Geology*, 257(1/2): 114–128.
- Jiang Y H, Zhao P, Zhou Q, Liao S Y, Jin G D. 2011. Petrogenesis and tectonic implications of Early Cretaceous S and A-type granites in the northwest of the Gan–Hang rift, SE China[J]. *Lithos*, 121: 55–73.
- Lapierre H, Jahn B M, Charvet J, Cddex R. 1997. Mesozoic felsic arc magmatism and continental olivine tholeiites in Zhejiang Province and their relationship with the tectonic activity in southeastern China[J]. *Tectonophysics*, 274: 321–338.
- Le Maitre R W. 2002. *Igneous Rocks: A Classification and Glossary of Terms*[M]. 2nd Edition. Cambridge University Press. 1–256.
- Li Xianhua. 2000. Cretaceous magmatism and lithospheric extension in southeast China[J]. *Journal of Asian Earth Science*, 18: 293–305.
- Li Xianhua, Li Zhengxiang, Li Wuxian, Liu Ying, Yuan Chao, Wei Gangjian, Qi Changshi. 2007. U–Pb zircon, geochemical and Sr–Nd–Hf isotopic constraints on age and origin of Jurassic I– and A-type granites from central Guangdong, SE China: A major igneous event in response to foundering of a subducted flat–slab[J]. *Lithos*, 96:186–204.
- Li Xianhua, Li Wuxian, Wang Xuance, Li Qiuli, Tang Guoqiang. 2009. Role of Mantle-Derived Magma in Genesis of Early Yanshanian Granites in the Nanling Range, South China: In Situ Zircon Hf–O Isotopic Constraints[J]. *Science in China(Series D)*, 52(9): 1262–1278.
- Li Xianhua, Li Wuxian, Li Qiuli, Wang Xuance, Liu Yu, Yang Yueheng. 2010. Petrogenesis and Tectonic Significance of the ~850Ma Gangbian Alkaline Complex in South China: Evidence from In Situ Zircon U–Pb Dating, Hf–O Isotopes and Whole-Rock Geochemistry[J]. *Lithos*, 114(1/2): 1–15.
- Li Zhengxiang, Li Xianhua. 2007. Formation of the 1300 km-wide intracontinental orogen and post-orogenic magmatic province in Mesozoic South China: A flat–slab subduction model[J]. *Geology*, 35: 179–182.
- Ludwig K R. 2001. *Squid 1.02: A User’s Manual*. Berkeley[M]. Berkeley: Geochronology Centre Special Publication, 1–19.
- Mao Jingwen, Chen Maohong, Yuan Shunda, Guo Chunli. 2011. Geological characteristics of the Qinhang(or Shihang) metallogenetic belt in South China and spatial-temporal distribution regularity of mineral deposits[J]. *Acta Geologica Sinica*, 85(5): 636–658(in Chinese with English abstract).
- Martin H, Bonin B, Capdevila R, Jahn B M, Lameyre J, Wang Y. 1994. The Kuiqi peralkaline granitic complex (SE China): Petrology and geochemistry[J]. *J. Petrol.* 35 983–1015.
- Meng Xiangjin, Dong Guangyu, Liu Jianguang. 2007. *Lengshuikeng Porphyry Pb–Zn–Ag deposit in Jiangxi Province*[M]. Beijing: Geological Publishing House, 1–148(in Chinese).
- Meng Xiangjin, Hou Zengqian, Dong Guangyu, Liu Jianguang, Zuo Liyan, Yang Zhusen, Xiao Maozhang. 2009. Geological characteristics and mineralization timing of the Lengshuikeng porphyry Pb–Zn–Ag deposit, Jiangxi Province[J]. *Acta Geologica Sinica*, 83(12): 1951–1967(in Chinese with English abstract).
- Meng Xiangjin, Xu Wenyi, Yang Zhusen, Hou Zengqian, Li Zhenqing, Yu Yushuai, Xiao Maozhang, He Xirong, Wan Haozhang. 2012. Time limit of volcanic–magmatic action in Lengshuikeng orefield, Jiangxi: Evidence from SHRIMP zircon U–Pb ages[J]. *Mineral Deposits*, 31(4): 831–838(in Chinese with English abstract).
- Mojzsis S J, Harrison T M, Pidgeon R T. 2001. Oxygen–Isotope Evidence from Ancient Zircons for Liquid Water at the Earth’s Surface 4300Myr Ago[J]. *Nature*, 409(6817): 178–181.
- Müller D, Rock N M S, Groves D I. 1992. Geochemical discrimination between shoshonitic and potassic volcanic rocks in different tectonic settings: A pilot study[J]. *Mineralogy and Petrology*, 46(4):

- 259–289.
- Nasdala L, Hofmeister W, Norberg N, Martinson J M, Corfu F, Dörr W, Kamo S L, Kennedy A K, Kronz A, Reiners P W, Frei D, Kosler J, Wan Y, Götze J, Häger T, Kröner A and Valley J W. 2008. Zircon M257: A homogeneous natural reference material for the ion microprobe U– Pb analysis of zircon[J]. *Geostandards and Geoanalytical Research*, 32(3): 247–265.
- O’Neil J R O, Chappell B W J. 1977. Oxygen and Hydrogen Isotope Relations in the Berridale Batholith[J]. *Journal of the Geological Society*, 133(6): 559–571.
- Pearce J A, Harris N B W, Tsigas A G. 1984. Trace element discrimination diagrams for the tectonic interpretation of granitic rocks[J]. *Journal of Petrology*, 25: 956–983.
- Peck W H, Valley J W, Wilde S A, Graham C M. 2001. Oxygen Isotope Ratios and Rare Earth Elements in 3.3 to 4.4 Ga Zircons: Ion Microprobe Evidence for High $\delta^{18}\text{O}$ Continental Crust and Oceans in the Early Archean[J]. *Geochemistry et Cosmochimica Acta*, 65(22): 4215–4229.
- Pu Wei, Zhao Kuidong, Ling Hongfei, Jiang Shaoyong. 2004. High precision Nd isotope measurement by Triton TI mass spectrometry[J]. *Acta Geoscientica Sinica*, 25(2): 271–274(in Chinese with English abstract).
- Pu Wei, Gao Jianfeng, Zhao Kuidong, Ling Hongfei, Jiang Shaoyong. 2005. Separation method of Rb–Sr, Sm–Nd using DCTA and HIBA[J]. *Journal of Nanjing University(Natural Sciences)*, 41(4): 445–450(in Chinese with English abstract).
- Qiu Junting, Yu Xinqi, Wu Ganguo, Liu Jiangguang, Xiao Maozhang. 2013. Geochronology of igneous rocks and nappe structures in Lengshuikeng deposit, Jiangxi Province, China[J]. *Acta Petrologica Sinica*, 29(3): 812–826(in Chinese with English abstract).
- Rogers G, Hawkesworth C J. 1989. A geochemical traverse across the North Chilean Andes: Evidence for crust generation from the mantle wedge[J]. *Earth and Planetary Science Letters*, 91(3/4): 271–285.
- Stern R J. 2002. Subduction zones[J]. *Reviews of Geophysics*, 40(4): 1–38.
- Su Huimin, Mao Jingwen, He Xirong, Lu Ran. 2013. Timing of the formation of the Tianhuashan Basin in northern Wuyi as constrained by geochronology of volcanic and plutonic rocks[J]. *Science China: Earth Sciences*, 56: 940–955.
- Sun S S, McDonough W F. 1989. Chemical and isotopic systematics of oceanic basalts: Implications for mantle composition and processes[J]. In: Saunders A D and Norry M J, eds. *Magmatism in the Ocean Basins*. Geological Society Special Publication. 313–345.
- Sylvester P J. 1998. Post-collisional strongly peraluminous granites[J]. *Lithos*, 45(1/4): 29–44.
- Tanaka T, Togashi S, Kamioka H, Amakawa H, Kagami H, Hamamoto T, Yuhara M, Orihashi Y, Yoneda S, Shimizu H, Kunimaru T, Takahashi K, Yanagi T, Nakano T, Fujimaki H, Shinjo R, Asahara Y, Tanimizu M, Dragusanu C. 2000. JNdI-1: A neodymium isotopic reference in consistency with LaJolla neodymium[J]. *Chemical Geology*, 168: 279–281.
- Taylor S R, McLennan S M. 1985. *The Continental Crust: Its Composition and Evolution*[M]. Oxford: Blackwell Scientific Publication, Carlton, 1–312.
- Tu Guangchi. 1989. *Lead–Zinc Deposit in China, Chinese Deposit (Volume 1)*[M]. Beijing: Geological Publishing House, 116–204(in Chinese).
- Valley J W, Lackey J S, Cavosie A J, Clechenko C C, Spicuzza M J, Basei M A S, Bindeman I N, Ferreira V P, Sial A N, King E M, Peck W H, Sinha A K, Wei C S. 2005. 4.4 Billion Years of Crustal Maturation: Oxygen Isotope Ratios of Magmatic Zircon[J]. *Contributions to Mineralogy and Petrology*, 150(6): 561–580.
- Wang Changming, Xu Yigan, Wu Ganguo, Zhang Da, Yang Lei, Liu Jiangguang, Wan Haozhang, Di Yongjun, Yu Xinqi, He Mingyue, Zhang Yaoyao. 2011. C, O, S and Pb isotopes characteristics and sources of the ore metals of the Lengshuikeng Ag–Pb–Zn ore field, Jiangxi[J]. *Earth Science Frontiers*, 18(1): 179–193(in Chinese with English abstract).
- Wang Changming, Zhang Da, Wu Ganguo, Xu Yigan, Carranza E J M, Zhang Yaoyao, Li Huaikun, Geng Jianzhen. 2013. Zircon U–Pb geochronology and geochemistry of rhyolitic tuff, granite porphyry and syenogranite in the Lengshuikeng ore district, SE China: Implications for a continental arc to intra-arc rift setting[J]. *Journal of Earth System Science*, 122(3): 809–830.
- Wang Changming, Zhang Da, Wu Ganguo, Santosh M, Zhang Jing, Xu Yigan, Zhang Yaoyao. 2014. Geological and isotopic evidence for magmatic–hydrothermal origin of the Ag–Pb–Zn deposits in the Lengshuikeng District, east-central China[J]. *Miner Deposita*, 49: 733–749.
- Wang Dezi, Liu Changshi, Shen Weizhou, Chen Fanrong. 1993. The Contrast between Tonglu I-type and Xiangshan S-type clastoporphyritic lava[J]. *Acta Petrologica Sinica*, 9(1): 44–54(in Chinese with English abstract).
- Weis D, Kieffer B, Maerschalk C, Barling J, Jong J, Williams G A, Hanano D, Pretorius W, Mattielli N, Scoates J S, Goolaerts A, Friedman R M, Mahoney J B. 2006. High-precision isotopic characterization of USGS reference materials by TIMS and MC-ICP-MS[J]. *Geochemistry, Geophysics, Geosystems*, 7(8): 1525–2027.
- Williams I S. 1998. U–Th–Pb Geochronology by Ion Microprobe. In: McKibben M A, Shanks W C and Ridley W I(eds.). *Applications of Microanalytical Techniques to Understanding Mineralizing Processes*[J]. *Reviews in Economic Geology*, 7: 1–35.
- Wilson M. 1989. *Igneous Petrogenesis: A Global Tectonic Approach*[M]. London: Unwin Hyman, 1–468.
- Wu Fuyuan, Li Xianhua, Yang Jinhui, Zheng Yongfei. 2007a.

- Discussions on the petrogenesis of granites[J]. *Acta Petrologica Sinica*, 23(6): 1217–1238(in Chinese with English abstract).
- Wu Fuyuan, Li Xianhua, Zheng Yongfei, Gao Shan. 2007b. Lu-Hf isotopic systematics and their applications in petrology[J]. *Acta Petrologica Sinica*, 23(2): 185–220(in Chinese with English abstract).
- Xie X, Xu X S, Zou H B, Jiang S Y, Zhang M and Qiu J S. 2006. Early J2 basalts in SE China: Incipience of largescale late Mesozoic magmatism[J]. *Sci. China Ser. D*, 49: 796–815.
- Yu Minggang, Zhao Xilin, Qian Maiping, Duan Zheng, Zhang Xuehui, Wan Haozhang, Xiao Maozhang, Sun Jiandong. 2015. The discovery of Late Jurassic volcanic rocks in Lengshuikeng, Jiangxi and their geological significance[J]. *Rack and Mineral Analysis*, 34 (1): 138–149(in Chinese with English abstract).
- Zuo Liyan, Hou Zengqian, Meng Xiangjin, Yang Zhiming, Song Yucai, Li Zheng. 2010. SHRIMP U-Pb zircon geochronology of the ore-bearing rock in the Lengshuikeng porphyry type Ag-Pb-Zn deposit[J]. *Geology in China*, 37(5): 1450–1456(in Chinese with English abstract).
- Zhou Qing, Jiang Yaohui, Zhao Peng, Liao Shiyong, Jin Guodong. 2012. Origin of the Dexing Cu-bearing porphyries, SE China: Elemental and Sr-Nd-Pb-Hf isotopic constraints[J]. *International Geology Review*, 54(5): 572–592.
- Zhou Xinmin, Li Wuxian. 2000. Origin of Late Mesozoic rocks in southeastern China: Implications for lithosphere subduction and underplating of mafic magmas[J]. *Tectonophys*, 326(3/4): 269–287.
- ### 附中文参考文献
- 高山,骆庭川,张本仁,张宏飞,韩吟文,赵志丹,Hartmut Kern. 1999. 中国东部地壳的结构和组成[J]. *中国科学(D辑)*,29(3):204–213.
- 韩吟文,马振东. 2003. 地球化学[M]. 北京:地质出版社. 1–370.
- 何细荣,黄冬如,饶建锋. 2010. 江西贵溪冷水坑矿田下鲍银铅锌矿床地质特征及成因探讨[J]. *中国西部科技*, 9(25): 1–3.
- 侯可军,李延河,邹天人,曲晓明,时雨若,谢桂青. 2007. LA-MC-ICP-MS 锆石Hf同位素的分析方法及地质应用[J]. *岩石学报*, 29 (11): 3968–3980.
- 毛景文,陈懋弘,袁顺达,郭春丽. 2011. 华南地区钦杭成矿带地质特征和矿床时空分布规律[J]. *地质学报*, 85(5): 636–658.
- 孟祥金,董光裕,刘建光. 2007. 江西冷水坑斑岩型铅锌银矿床[M]. 北京:地质出版社, 1–148.
- 孟祥金,侯增谦,董光裕,刘建光,左力艳,杨竹森,肖茂章. 2009. 江西冷水坑斑岩型铅锌银矿床地质特征、热液蚀变与成矿时限[J]. *地质学报*, 83(12): 1951–1967.
- 孟祥金,徐文艺,杨竹森,侯增谦,李振清,于玉帅,肖茂章,何细荣,万浩章. 2012. 江西冷水坑矿田火山-岩浆活动时限:SHRIMP锆石U-Pb年龄证据[J]. *矿床地质*, 2012, 31(4): 831–838.
- 濮巍,赵葵东,凌洪飞,蒋少涌. 2004. 新一代高精度高灵敏度的表面热电离质谱仪(Triton TI)的Nd同位素测定[J]. *地球学报*, 25(2): 271–274.
- 濮巍,高剑峰,赵葵东,凌洪飞,蒋少涌. 2005. 利用DCTA和HIBA快速有效分离Rb-Sr-Sm-Nd的方法[J]. *南京大学学报(自然科学)*, 41(4): 445–450.
- 邱骏挺,余心起,吴淦国,刘建光,肖茂章. 2013. 江西冷水坑矿区构造-岩浆活动的年代学约束[J]. *岩石学报*, 29(3): 812–826.
- 苏慧敏,毛景文,何细荣,卢燃. 2013. 北武夷天华山盆地形成时限的约束:来自火山岩-侵入岩的年代学证据[J]. *中国科学:地球科学*, 43(5): 745–759.
- 涂光炽. 1989. 中国铅锌矿床. *中国矿床(上册)* [M]. 北京:地质出版社, 116–204.
- 王长明,徐贻赣,吴淦国,张达,杨磊,刘建光,万浩章,狄永军,余心起,何明跃,张垚垚. 2011. 江西冷水坑Ag-Pb-Zn矿田碳氧硫铅同位素特征及成矿物质来源[J]. *地学前缘*, 18(1): 179–193.
- 王德滋,刘昌实,沈渭洲,陈繁荣. 1993. 桐庐I型和相山S型两类碎斑熔岩对比[J]. *岩石学报*, 9(1): 44–54.
- 吴福元,李献华,郑永飞,高山. 2007. Lu-Hf同位素体系及其岩石学应用[J]. *岩石学报*, 23(2): 185–220.
- 余明刚,赵希林,钱迈平,段政,张雪辉,万浩章,肖茂章,孙建东. 2015. 江西冷水坑火山-侵入杂岩LA-ICP-MS 锆石U-Pb年龄及地质意义[J]. *岩矿测试*, 34(1): 138–149.
- 左力艳,侯增谦,孟祥金,杨志明,宋玉财,李政. 2010. 冷水坑斑岩型银铅锌矿床含矿岩体锆石SHRIMP U-Pb年代学研究[J]. *中国地质*, 37(5): 1450–1456.
- 周建祥. 2009. 冷水坑矿田层控叠生型矿体特征及成因[J]. *民营科技*, 12: 4–6.